

# RELATIONSHIP OF ALUMINUM GRAIN SIZE TO THE GRAIN SIZE OF POLYCRYSTALLINE SILICON PRODUCED BY THE ALUMINUM INDUCED CRYSTALLIZATION OF AMORPHOUS SILICON

Emilio Stinzianni, Kathleen Dunn, Zhao Zhouying, Manisha Rane-Fondacaro, Harry Efstathiadis, and Pradeep Haldar

Energy and Environmental Applications Center (E2TAC)  
College of Nanoscale Science and Engineering  
University at Albany, State University of New York

## ABSTRACT

The aluminum-induced crystallization and layer exchange process shows great promise for converting a-Si into large-grained poly-Si for solar cell applications. To investigate the relationship between the grain size of Al and the final grain size of poly-Si, a series of samples were deposited by RF magnetron sputtering 165 nm of Al onto SiN/SiO<sub>2</sub> coated (100) silicon substrates. The Al grain size was varied by vacuum annealing prior to the deposition of 195 nm of a-Si. Completion of the layer exchange process resulted in poly-Si films which were then characterized with plan view TEM. The average Si grain size was found to increase as a function of increasing Al grain size, consistent with the grain-boundary nucleation model for this process. The largest average Si grain size of  $4.9 \pm 1.92 \mu\text{m}$  corresponded to the Al sample which was annealed for 24 hours at 550°C. The microstructure of the poly-Si film can therefore be manipulated by altering the properties of the as-deposited Al layer with an isothermal anneal.

## INTRODUCTION

Thin films of polycrystalline silicon (poly-Si) are a promising candidate for solar cell applications because of a combination of advantages. Like amorphous-silicon (a-Si) thin films, poly-Si can be deposited onto a foreign substrate (e.g. glass) which reduces raw material utilization and enables use in wide variety of applications. In addition, poly-Si films have a higher carrier mobility than amorphous silicon films, enabling the use of thicker films to absorb more photons of light. Significant production challenges, however, still hamper widespread adoption of poly-Si thin films in solar cells applications [1]. In particular, excessive electron-hole pair recombination reduces the efficiency of the solar cell. To avoid this problem, the poly-Si absorber layer should be comprised of large grains with few intragrain defects. Traditional methods for reducing defect density (i.e. high temperature annealing) are to be avoided because most low-cost transparent substrates will not withstand this treatment. Over the past several decades, many approaches have been investigated to fabricate thin films of large-grained poly-Si [2] either by direct deposition (e.g., CVD [3] and PECVD [4,5]) or by the crystallization of an a-Si thin film

(e.g. laser crystallization [6], Solid Phase Crystallization (SPC) [7,8], and Metal Induced Crystallization (MIC) [9]). The direct deposition methods, however, result in a fine-grained microstructure (10-100nm) and some of the CVD processes require high temperatures [10]. Although the crystallization of an a-Si thin film using the SPC process can be conducted using lower temperatures (~600°C), the resulting silicon grain sizes are still small and the annealing times are too long for large scale mass production. On the other hand, laser crystallization and MIC of a-Si have been shown to produce silicon grain sizes greater than one micrometer in diameter. Unfortunately, laser crystallization is not a low temperature process, either, and has a low throughput when large area films are to be produced. However, the MIC method is not only a low temperature process but also results in sufficiently high growth rates.

For the MIC growth process, a metal film is deposited in direct contact with the a-Si layer and then the two films are annealed resulting in poly-Si formation. The advantage that the MIC process has over other growth processes is that certain metals will lower the crystallization temperature of silicon and accelerate the rate of grain growth compared. Several different metals have been investigated for use in the MIC process (e.g. aluminum [11,12], cobalt [13], nickel [11,13], molybdenum [11], titanium [11], and gold [14]). Aluminum is particularly attractive for solar cell applications because it does not form a silicide, and thus the resulting poly-Si film could be used as a seed layer for additional a-Si crystallization [15-17]. The Al also dopes the Si film p-type, which, although the resulting doping concentration is too high ( $3 \times 10^{19} \text{ cm}^{-3}$ ) [18] for the poly-Si film to be used directly as an absorber layer, it would be appropriate for use as a back surface field for the solar cell. The literature now contains several reports on the Aluminum-Induced Crystallization of a-Si (AIC) process [19-22]. Of particular interest is the finding that the Al and a-Si films can exchange position in a film stack during a sub-eutectic (577°C) anneal, if the a-Si is at least as thick as the Al onto which it is deposited. It has been theorized that this exchange occurs via grain boundary diffusion, with nucleation of Si grains occurring at the grain boundaries in the Al template after Si segregation exceeds the solubility limit. After the exchange, a poly-Si film is in direct contact with the substrate, while the aluminum has been displaced to the surface of the poly-Si. This surface

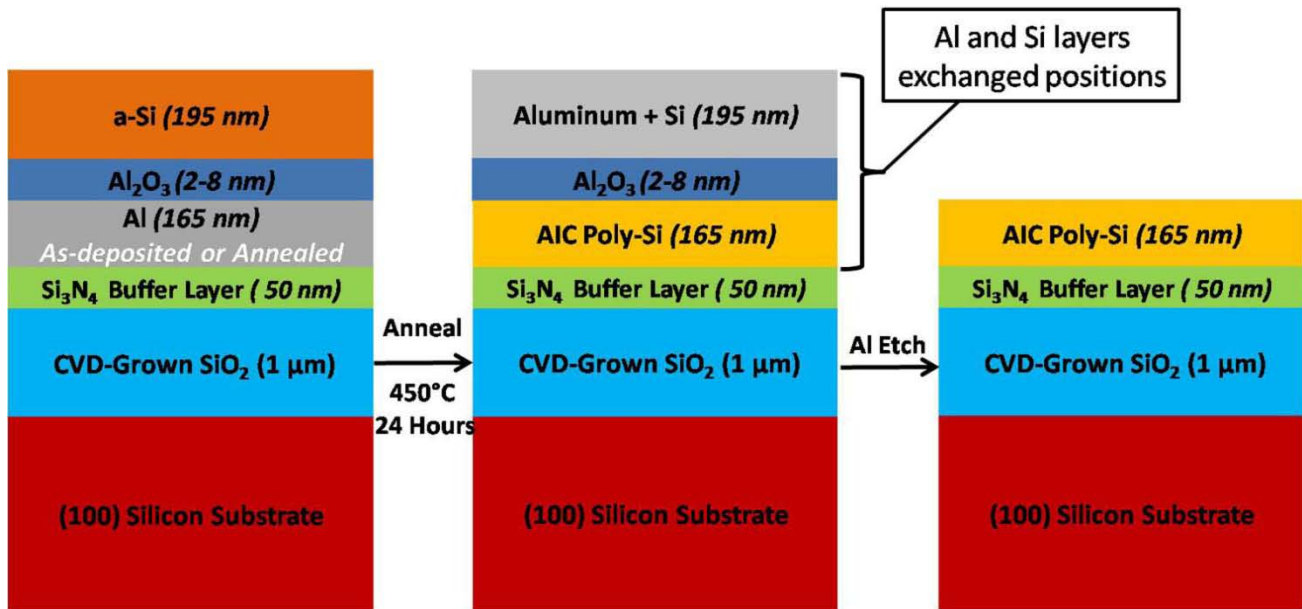


Fig. 1. Cross-sectional depiction of the aluminum induced crystallization of a-Si, layer exchange process.

layer of aluminum can then be removed via a selective wet-chemical etch.

Several factors are likely to influence the size of silicon grains made by the AIC layer exchange process, including the structural properties of the Al layer prior to stack annealing, the presence of an oxide layer between the Al and amorphous silicon, the anneal temperature, and the anneal duration.

This report investigates the relationship between the initial Al grain size and the resulting poly-Si grain size. In particular, the aluminum grain size is manipulated by annealing prior to the a-Si deposition, with the assumption that a reduction in grain boundary nucleation sites will result in larger Si grain size in the final film.

## EXPERIMENTAL

The substrates used for the depositions were (100) silicon wafers with 1 micron of CVD-grown SiO<sub>2</sub> and 50 nm of RF magnetron-sputtered (13.56 MHz, 3.4 Watts/cm<sup>2</sup>) Si<sub>3</sub>N<sub>4</sub> which acts as a diffusion barrier. For the Al grain size investigation, a 165 nm thick film of Al was RF magnetron-sputtered (13.56 MHz, 3.4 Watts/cm<sup>2</sup>) on a single substrate. The wafer was cleaved and coupons were separately vacuum-annealed (~4.0x10<sup>-4</sup> Torr) at either 500°C or 550°C for 24 h using a ramp-up rate of 10°C/min and a ramp-down rate of ~3°C/min back to room temperature. Plan-view transmission electron microscopy (TEM) specimens were prepared from the aluminum films by conventional grinding, polishing, dimpling, and argon ion milling at 5 kV and 2 kV. The resulting specimens were imaged in a JEOL 200cx operated at 160 kV and the Al grain sizes were measured using the Gatan Digital Micrograph software package.

For the AIC poly-Si grain size analysis, a separate deposition of 165 nm thick Al was RF magnetron sputtered and allowed to oxidize in air for 20 hours to allow for the formation of an Al<sub>2</sub>O<sub>3</sub> layer. This oxide layer was needed to lower the diffusion rate of silicon into aluminum which in turn reduces the number of silicon nuclei that form during the subsequent anneal, resulting in larger silicon grains [23]. The time for the oxidation was chosen based on earlier reports [24]. After oxidation, the wafer was placed back into the sputtering chamber and a 195 nm thick a-Si layer was RF sputter deposited (13.56 MHz, 3.4 Watts/cm<sup>2</sup>), a layer thickness chosen to ensure that the layer exchange process will run to completion, forming a continuous poly-Si film. Additional samples were prepared with larger aluminum grain sizes by annealing a piece of the 165-nm aluminum films at either 500°C or 550°C for 24 h prior to the deposition of the a-Si. These annealed aluminum films were similarly allowed to oxidize in air for 20 hours before the 195 nm thick a-Si film was sputter-deposited. To complete the AIC process (schematically depicted in Fig. 1), pieces of all samples were vacuum annealed at 450°C for 24 hours. Cross-sectional TEM specimens were prepared from the samples after the AIC layer exchange process completed using a conventional ex-situ lift-out technique in a FEI Nova Nanolab 600 Dualbeam. The specimens were characterized by using a JEOL 2010F operated at 200kV, equipped with an EDAX Si-Li EDS detector

Additional samples were subjected to a wet etch to selectively remove the Al layer, consisting of 80% phosphoric acid, 10% DI water, 5% acetic acid, and 5% nitric acid at 55°C [18]. The morphology of the exposed poly-Si was investigated by plan view SEM in the FEI dualbeam and plan-view TEM specimens prepared manually for grain size analysis.

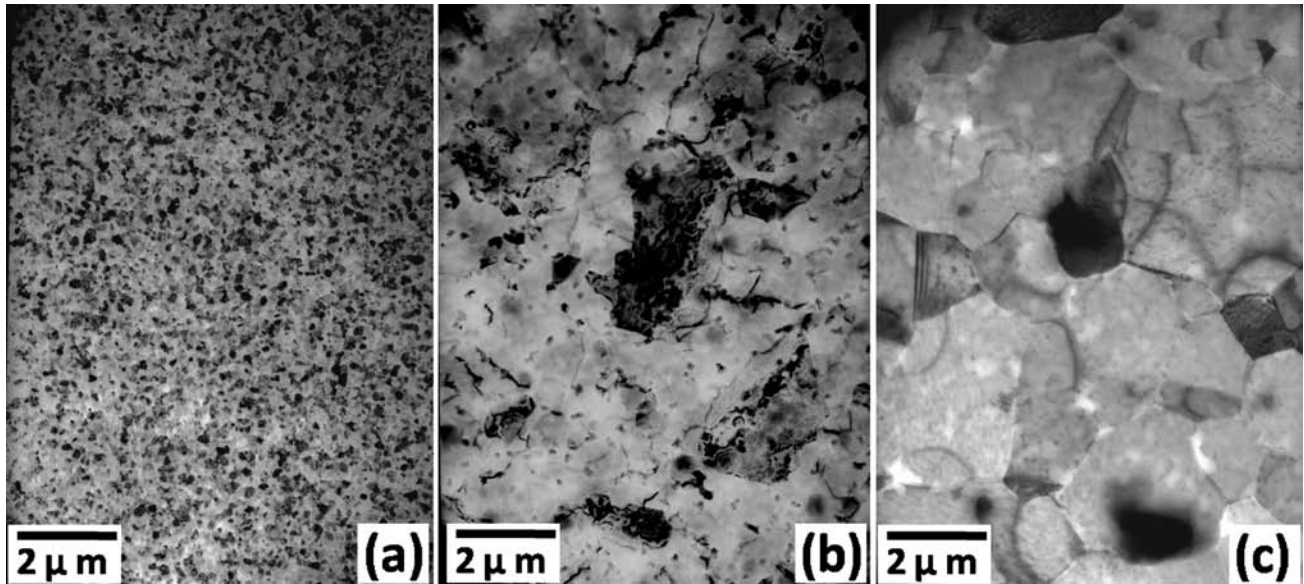


Fig. 2. TEM plan view micrographs of the aluminum films (a) As-deposited aluminum (b) Aluminum which was annealed at 500°C for 24 h (c) Aluminum film which was annealed at 550°C for 24 h. The aluminum grain size increases with an increase in annealing temperature.

## RESULTS AND DISCUSSION

### Aluminum grain size

Fig. 2 presents plan-view TEM micrographs of the as-deposited and annealed Al films, while Fig. 3 displays this data graphically.

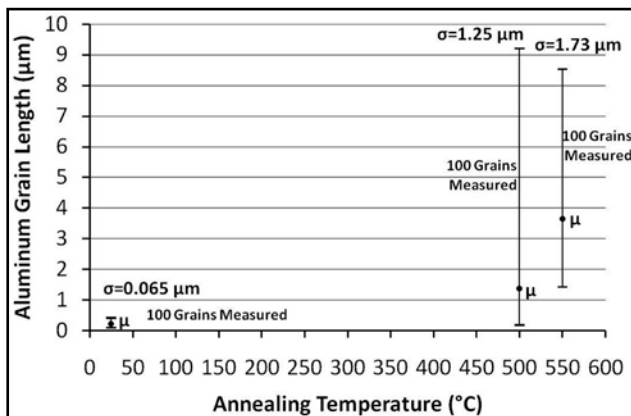


Fig. 3. Grain length measurements for the as-deposited and annealed aluminum films. The top and bottom of the bars represent the minimum and maximum measured grain lengths while the average of 100 measurements ( $\mu$ ), is plotted in the spread of the data. The calculated variances ( $\sigma$ ) are also reported.

The average of 100 individual grain diameter measurements for the as-deposited sample and for the samples annealed at 500°C and 550°C are  $0.212 \pm$

$0.065\mu\text{m}$ ,  $1.38 \pm 1.25\mu\text{m}$ , and  $3.65 \pm 1.73\mu\text{m}$ . The Al grain sizes increase with increasing temperature, with 550°C producing the largest average grain size. It should also be noted that an Al film was annealed at 600°C for 24 h; however the Al film did not survive this treatment and evaporated. It is unclear at this stage whether the large variance in the Al grain sizes will impede or assist the AIC process.

### AIC poly-Si films

After the AIC anneal was completed, X-ray diffraction  $\theta$ - $2\theta$  scans confirmed the presence of poly-Si. Fig. 4 shows the cross-sectional TEM image of the completed MIC film stack for the sample using as-deposited Al. EDS analysis of each of the individual layers indicates that the film adjacent to the  $\text{Si}_3\text{N}_4$  substrate is Si, whereas the layer above the Si consists of a mixture of nanocrystalline aluminum and silicon, embedded in a porous amorphous matrix. Near the surface, a Si-rich region persists as a residual of the excess a-Si deposited prior to the 450°C anneal. It should be noted that the poly-Si film likely contains a small amount of Al; however EDS is not sensitive enough to detect such a small quantity of dopant (EDS sensitivity  $\sim 0.2$  at. %). The uppermost layer visible in Fig. 4 is a thin layer of platinum deposited for surface protection during TEM specimen preparation in the dual beam FIB. Even with this protection, some damage is done to the top 20 nm of the film (mostly  $\text{Ga}^+$  ion implantation) visible as a dark, narrow band between the Pt and Si-rich layers. The polycrystalline structure of the Si layer on top of the  $\text{Si}_3\text{N}_4$  in Fig. 4 was confirmed with dark field TEM imaging and selected area diffraction patterns.

After Al etching, the poly-Si films surface morphology was examined by SEM (see Fig. 5). All films had Si islands as well as etch pits due to the removal of Al grains which remained protruding into the poly-Si even after the AIC treatment.

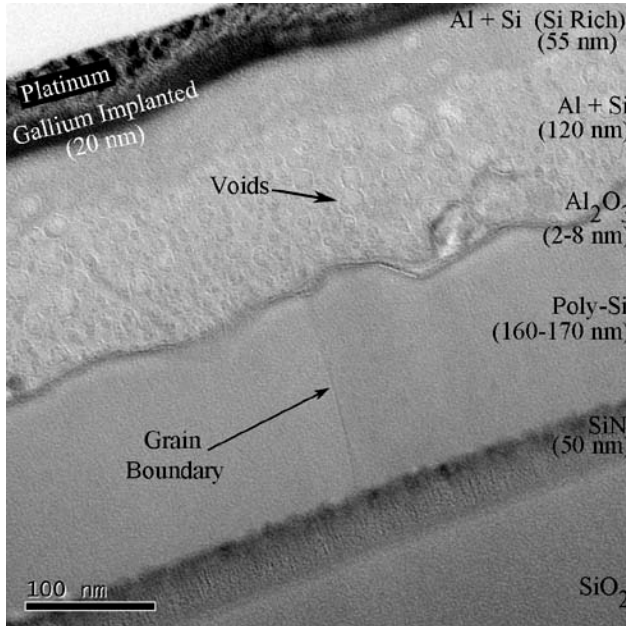


Fig. 4. Cross-sectional TEM image of the completed sample that used an as-deposited Al film for the AIC anneal at 450°C. The Al and Si layers have exchanged positions and the silicon is now adjacent to the SiN substrate and has been crystallized into poly-Si.

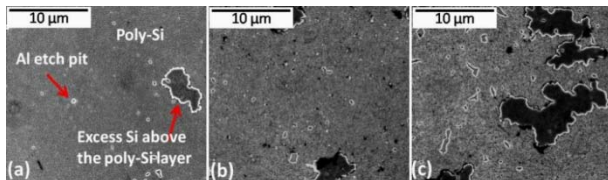


Fig. 5. SEM plan view images of the AIC produced poly-Si films fabricated using (a) an as-deposited aluminum film; (b) an aluminum film that was vacuum annealed at 500°C for 24 h; and (c) aluminum film that was vacuum annealed at 550°C for 24 h. All of the poly-Si films contain aluminum etch pits and islands of silicon on top of the poly-Si layer.

The etch pit density per 2500µm<sup>2</sup> area did not vary significantly between the samples (see Fig. 6). However, the average length of the etch pits in the sample that had the largest Al grain size (Al annealed at 550°C) was about 200nm greater than the one that had smaller Al grain

sizes. In addition, there are islands present on top of the poly-Si layer and were confirmed to be Si by EDS and result from the excess quantity of a-Si deposited before stack annealing. These islands are as undesirable as the Al etch pits are for solar cell applications; in that case the thicknesses of the Al and a-Si layers would need to be balanced to minimize these effects.

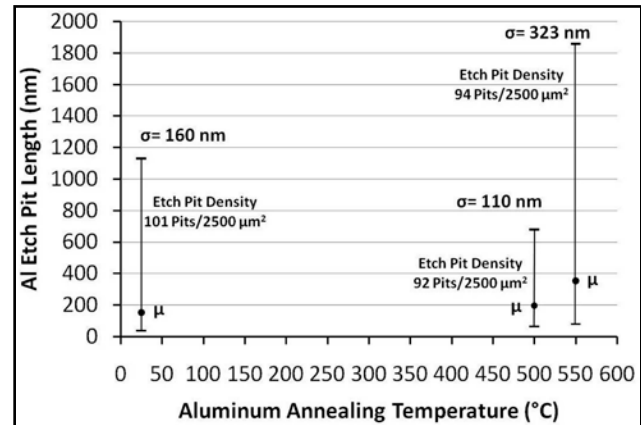


Fig. 6. Etch pit length for the poly-Si films as a function of Al pre-treatment. The top and bottom of the bars represent the minimum and maximum measured etch pit length while the average etch pit length ( $\mu$ ), is plotted in the spread of the data. The calculated variances ( $\sigma$ ), and the etch pit density per 2500µm<sup>2</sup>, are also reported.

The plan view TEM micrographs of the 3 cases from the study after the Al etches are presented in Fig. 7. From the micrographs, many Si grains are visible in addition to holes which occur where the Al etch pits intersect the TEM specimen plane. To unambiguously determine the location of grain boundaries, a series of micrographs were recorded at several values of specimen tilt (up to  $\pm 20^\circ$ ) to account for diffraction effects. The length of 50 individual grains were averaged for each sample, with the size increasing from  $2.1 \pm 0.081\mu\text{m}$  in the sample using as-deposited Al, to  $4.2 \pm 2.25\mu\text{m}$  and  $4.8 \pm 1.95\mu\text{m}$  for the samples whose Al layer had been annealed at 500° and 550°C, respectively (see Fig. 8). These results are consistent with the model of poly-Si nucleation at Al grain boundaries [18, 25] and for Si grain size values reported in the literature [12,18]. Once nucleated, the Si grains continue to grow until they entirely displace the host Al, with growth terminating when two Si grains impinge on one other. A large Al grain size is therefore desirable to the low number of Si nuclei which form, and increasing their separation from each other, leading to a larger final Si grain size.

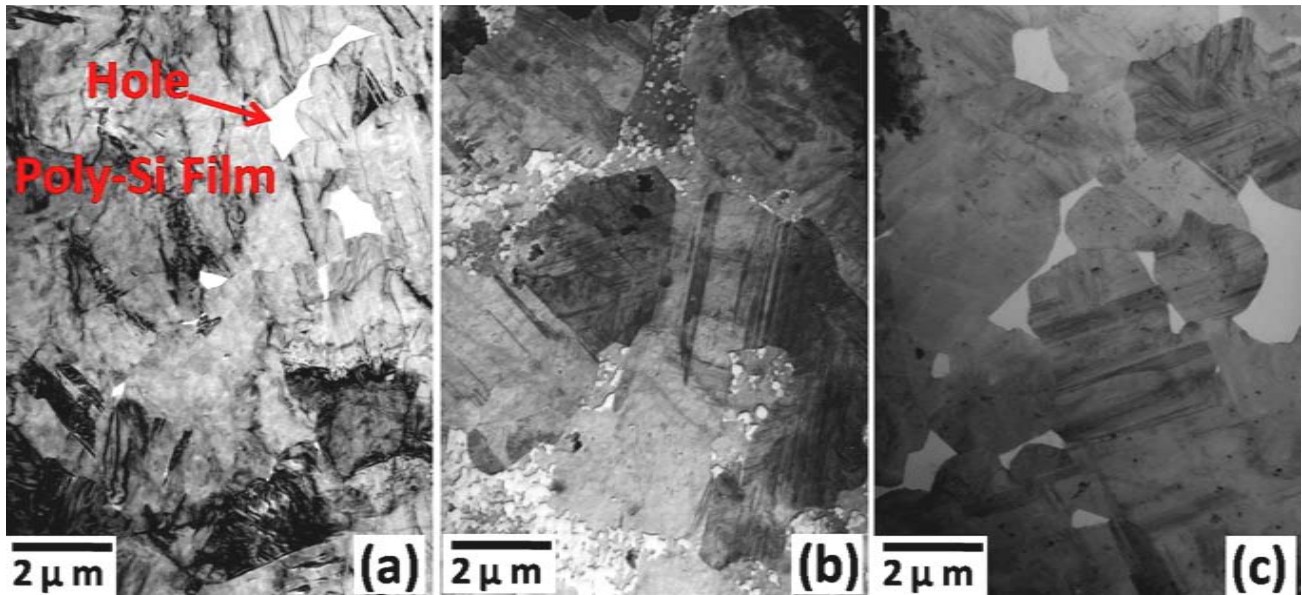


Fig. 7. Plan view TEM micrographs of the poly-Si films fabricated using (a) an as-deposited aluminum film; (b) an aluminum film vacuum annealed at 500°C for 24 h; and (c) an aluminum film vacuum annealed at 550°C for 24 h. All of the TEM samples contain holes which result from the intersection of an Al etch pit with the plane of the TEM specimen.

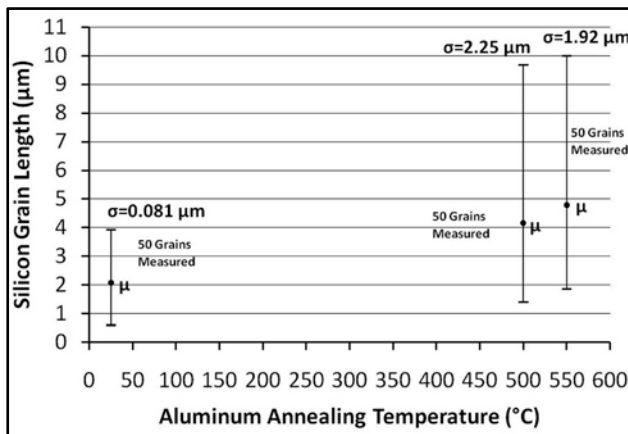


Fig. 8. Grain length measurements for 3 poly-Si films fabricated using different aluminum grain sizes. The top and bottom of the bars represent the minimum and maximum measured grain lengths while the mean of 50 measurements ( $\mu$ ), is plotted in the spread of the data. The calculated variances ( $\sigma$ ) are also reported.

### CONCLUSION

The relationship between the size of aluminum grains and the size of polycrystalline silicon grains produced by the aluminum induced crystallization layer exchange process of amorphous silicon was investigated by enlarging the aluminum grains with an anneal prior to the deposition of the a-Si layer. The average silicon grain

size increased when aluminum films with larger grains were used for the crystallization. Thus, enlarging aluminum grain size prior to the deposition of the a-Si and completion of the AIC process is beneficial for polycrystalline silicon films that are intended to be used in solar cell applications to reduce electron hole pair recombination and increase the efficiency of the solar cell.

### REFERENCES

- [1] B. Zebentout, Z. Benamara, and T. Mohammed-Brahim, "Dependence of photovoltaic parameters on grain size and density of states in  $n^+i-p^+$  and  $p^+i-n^+$  polycrystalline solar cells", *Thin Solid Films* **516**, 2007, pp. 84-90.
- [2] A.G. Aberle, "Fabrication and characterization of crystalline silicon thin-film materials for solar cells", *Thin Solid Films* **511-512**, 2006, pp. 26-34.
- [3] C. Lim, Jungwoo Lee, and Junichi Hanna, "Nucleation and growth of poly-Si films deposited directly on glass substrate in reactive thermal-chemical vapor deposition", *Thin Solid Films* **517**, 2009, pp. 2627-2632.
- [4] S. Hasegawa, M. Sakata, T. Inokuma, and Y. Kurata, "Effects of deposition temperature on polycrystalline silicon films using plasma-enhanced chemical vapor deposition", *J. Appl. Phys.* **84**, No.1, 1998, pp. 584-588.

- [5] T. Matsui, M. Tsukiji, H. Saika, T. Toyama, and H. Okamoto, "Correlation between microstructure and photovoltaic performance of polycrystalline silicon thin film solar cells", *Jpn. J. Appl. Phys.* **41**, Part 1, No.1, 2002, pp. 20-27.
- [6] G. Andrä, J. Bergmann, and F. Falk, "Laser crystallized multicrystalline silicon thin films on glass", *Thin Solid Films* **487**, 2005, pp. 77-80.
- [7] D. Song, D. Inns, A. Straub, M. L. Terry, P. Campbell, A. G. Aberle, "Solid phase crystallized polycrystalline thin-films on glass from evaporated silicon for photovoltaic applications", *Thin Solid Films* **513**, 2006, pp. 356-363.
- [8] C. Becker, E. Conrad, P. Dogan, F. Fenske, B. Gorke, T. Hänel, K.Y. Lee, B. Rau, F. Ruske, T. Weber, M. Berginski, J. Hüpkes, S.Gall, and B. Rech, "Solid-phase crystallization of amorphous silicon on ZnO:Al for thin-film solar cells", *Solar Energy Materials & Solar Cells* **93**, 2009, pp. 855-858.
- [9] J.H. Choi, D.Y. Kim, S.S. Kim, S.J. Park, and J. Jang, "Polycrystalline silicon prepared by metal induced crystallization", *Thin Solid Films* **440**, 2003, pp. 1-4.
- [10] A. Slaoui, S. Bourdais, G. Beaucarne, J. Poortmans, S. Reber, "Polycrystalline silicon solar cells on mullite substrates", *Solar Energy Materials & Solar Cells* **71**, 2002, pp. 245-252.
- [11] L. Pereira, H. Águas, R.M.S. Martins, P. Vilarinho, E. Fortunato, and R. Martins, "Polycrystalline silicon obtained by metal induced crystallization using different metals", *Thin Solid Films* **451-452**, 2004, pp. 334-339.
- [12] E. Pihan, A. Slaoui, and C. Maurice, "Growth kinetics and crystallographic properties of polysilicon thin films formed by aluminum-induced crystallization", *J. of Crystal Growth* **305**, 2007, pp. 88-98.
- [13] J. Kim, and W.A. Anderson, "Metal silicide-mediated microcrystalline silicon thin-film growth for photovoltaics", *Solar Energy Materials & Solar Cells* **91**, 2007, pp. 534-538.
- [14] L. Pereira, H. Águas, R.M. Martins, E. Fortunato, and R. Martins, "Polycrystalline silicon obtained by gold metal induced crystallization", *J. of Non-Crystalline Solids* **338-340**, 2004, pp. 178-182.
- [15] F. Liu, M.J. Romero, K.M. Jones, A.G. Norman, M.M. Al-Jassim, D. Inns, A.G. Aberle, "Intragrain defects in polycrystalline silicon thin-film solar cells on glass by aluminum induced crystallization and subsequent epitaxy", *Thin Solid Films* **516**, 2008, pp. 6409-6412.
- [16] S. Gall, J. Schneider, J. Klein, K. Hübener, M. Muske, B. Rau, E. Conrad, I. Sieber, K. Petter, K. Lips, M. Stöger-Pollach, P. Schattschneider, and W. Fuhs, "Large-grained polycrystalline silicon on glass for thin-film solar cells", *Thin Solid Films* **511-512**, 2006, pp. 7-14.
- [17] P.I. Widenborg, A. Straub, A.G. Aberle, "Epitaxial thickening of AIC poly-Si seed layers on glass by solid phase epitaxy", *J. of Crystal Growth* **276**, 2005, pp. 19-28.
- [18] O. Nast, and S.R. Wenham, "Elucidation of the layer exchange mechanism in the formation of polycrystalline silicon by aluminum-induced crystallization", *J. Appl. Phys.* **88**, No.1, 2000, pp. 124-132.
- [19] J. Klein, J. Schneider, M. Muske, S. Gall, and W. Fuhs, "Aluminum-induced crystallization of amorphous silicon: influence of the aluminum layer on the process", *Thin Solid Films* **451-452**, 2004, pp. 481-484.
- [20] O. Nast, S. Brehme, S. Pritchard, A.G. Aberle, and S.R. Wenham, "Aluminum-induced crystallization of silicon on glass for thin-film solar cells", *Solar Energy Materials & Solar Cells* **65**, 2001, pp. 385-392.
- [21] T.L. Alford, P.K. Shetty, N.D. Theodore, N. Tile, D. Adams, and J.W. Mayer, "Nanocrystalline Si formation in the a-Si/Al system on polyimide and silicon dioxide substrates", *Thin Solid Films* **516**, 2008, pp. 3940-3947.
- [22] O. Nast, T. Puzzer, L.M. Koschier, A.B. Sproul, and S.R. Wenham, "Aluminum-induced crystallization of amorphous silicon on glass substrates above and below the eutectic temperature", *Appl. Phys. Lett.* **73**, No. 22, 1998, pp. 3214-3216.
- [23] O. Nast, and A.J. Hartmann, "Elucidation of the layer exchange mechanism in the formation of polycrystalline silicon by aluminum-induced crystallization", *J. Appl. Phys.* **88**, No.2, 2000, pp. 716-724.
- [24] J. Schneider, J. Klein, M. Muske, S. Gall, W. Fuhs, "Aluminum-induced crystallization of amorphous silicon: preparation effect on growth kinetics", *J. of Non-Crystalline Solids* **338-340**, 2004, pp. 127-130.
- [25] J. Schneider, A. Schneider, A. Sarikov, J. Klein, M. Muske, S.Gall, W. Fuhs, "Aluminum-induced crystallization: Nucleation and growth process", *J. of Non-Crystalline Solids* **352**, 2006, pp. 972-975.